INDIAN JOURNAL OF INDUSTRIAL AND APPLIED MATHEMATICS
Vol. 11, No. 1, Jan–June 2020, pp. 42–61
IndianJournals.com
DOI: 10.5958/1945-919X.2020.00004.3

A Spectral Simulation of Magnetohydrodynamic Convective Nanofluid Slip Flow with Newtonian Heating and Radiative Heat Transfer

R. Nandkeolyar[1*], B. K. Mahatha[2] and Ali J. Chamkha[3]
[1]Assistant Professor, Department of Mathematics, National Institute of Technology Jamshedpur, Jamshedpur-831014, India
[2]Assistant Professor, Amity School of Engineering and Technology, Amity University Jharkhand, Ranchi-834001, India
[3]Faculty of Engineering, Kuwait College of Science and Technology, Doha District, Kuwait
(*Corresponding author) Email id: *rajnandkeolyar@gmail.com, [2]bhupeshmahatha@gmail.com, [3]a.chamkha@kcst.edu.kw

Abstract: In this paper, we present a numerical analysis of natural convection boundary layer flow of a nanofluid over a stretching sheet under the influence of a variable magnetic field in the presence of nonlinear radiative heat transfer, hydrodynamic slip and Newtonian heating effects. The Brownian diffusion and thermophoresis effects are employed to describe the nanofluid flow model consisting of non-linear partial differential equations, which is transformed into a similarity form and then treated with the spectral local-linearization method (SLLM) to present an in-depth analysis of the flow and heat transfer characteristics of the fluid flow. The fluid flow problem finds applications in many engineering devices including geothermal heat source pump and in cooling of electronic devices and stretched wires.

Keywords: Magnetic field, nanofluid flow, natural convection, Newtonian heating, non-linear thermal radiation, velocity-slip.

NOMENCLATURE

A	Momentum-slip parameter	C_{f_x}	local skin-friction coefficient
a	constant associated with linear stretching	c	specific heat at constant pressure
B	applied magnetic field	C_w	wall nanoparticle volume fraction
Bi_x	local Biot number	C_∞	ambient nanoparticle volume fraction
C	nanoparticle volume fraction	D_B	Brownian diffusion coefficient
C_1	a dimensionless parameter	D_T	thermophoretic diffusion coefficient

f	dimensionless stream function
g	acceleration due to gravity
h_f	heat transfer coefficient
k	thermal conductivity of the base fluid
Le	Lewis number
M	magnetic parameter
N_1	hydrodynamic slip-factor
Nb	Brownian motion parameter
Nc	convective parameter
Nr	buoyancy ratio parameter
Nt	thermophoresis parameter
Nu_x	local Nusselt number
Pr	Prandtl number
q_m	wall mass flux
q_r	radiative heat transfer flux
q_w	wall heat flux
Ra_x	local Rayleigh number
Sh_x	local Sherwood number
T	nanofluid temperature
T_f	characteristic temperature
T_∞	ambient temperature of nanofluid
u	velocity component along x direction
U_w	stretching velocity of the sheet
v	velocity component along y direction
x	coordinate along the sheet
y	coordinate normal to the sheet
α	thermal diffusivity of base fluid
$\alpha*$	Rosseland's mean absorption coefficient
β	volumetric co-efficient of thermal expansion
η	similarity variable
λ	stretching parameter
μ	viscosity of the base fluid
ν	kinematic viscosity of the base fluid
ϕ	dimensionless nanoparticle volume fraction
ψ	stream function
ρ_f	density of the base fluid
ρ_{f_∞}	free-stream density of the base fluid
ρ_p	density of the nanoparticle
σ	electrical conductivity of the base fluid
$\sigma*$	Stefan-Boltzmann constant
τ	ratio of specific heat capacities
τ_w	surface shear stress
θ	dimensionless temperature
θ_r	temperature ratio parameter

1. INTRODUCTION

Nanofluids, i.e. fluids with suspended nano-sized particles, have become a central point of investigation during the last few years due to their applications in areas of fluid engineering, automobile engineering, nanotechnology, medical sciences, refrigeration, electronics engineering etc. Roughly speaking, nanofluids are fluids with some 1-100 nm sized nanoparticles mixed in it. Base fluids are in general water, ethylene glycol, lubricants, etc. whereas the nanoparticles are, in general, of metals such as silver (Ag), copper (Cu), gold (Au), metal oxides such as alumina (Al_2O_3), copper oxides (CuO) etc. Carbides, silica and carbon nanotubes are also being used as nanoparticles. The employment of nanoparticles in a base fluid significantly affects the heat transfer aspects of the base fluid. Choi [1] was the first to refer these fluids as nanofluids while later, it was shown by Choi et al. [2] that the inclusion of merely 1% by volume increases the heat transfer capabilities of the base fluid by about two times. The improvement of the heat transfer capabilities of the base fluid due to the presence of nanoparticles were also observed by Xuan and Li [3]. The study of nanofluid flow over a stretching sheet was initiated by Khan and Pop [4]. Their model describing the flow incorporated the Brownian diffusion and thermophoresis effects. After this remarkable study, several

researchers the theoretical investigation of nanofluid flows past a stretching sheet under different conditions and configurations. The flow of a nanofluid in the vicinity of a stagnation point towards a stretching sheet was investigated numerically using homotopy analysis method (HAM) by Mustafa et al. [5]. In this study, Mustafa et al. [5] observed that the nanofluid flow velocity is an increasing function of stretching/sinking parameter. Hassani et al. [6] also presented an analytical solution of the boundary layer nanofluid flow over a stretching sheet using HAM. The retarding influence of magnetic field on the boundary layer flows is a well known property which comes into the picture due to the generation of Lorentz force. An external magnetic field may act as a stabilizer in a turbulence and delay the boundary layer formation causing less generation of heat into the flow system. Magnetohydrodynamic flows in which we study interaction of magnetic field with the flow field are highly important for many industrial and engineering uses such as in MHD propulsion in a watercraft, MHD generator, MHD turbines etc. Thus the theoretical analysis of magnetohydrodynamic (MHD) boundary layer nanofluid flows were presented by several researchers. Hamad [7] obtained an exact solution for the problem of MHD convective flow and heat transfer of a nanofluid past a semi-infinite vertical stretching sheet. Ibrahim et al. [8] considered the Brownian diffusion and thermophoretic model to discuss the nanofluid model in the MHD flow and heat transfer in the vicinity of a stagnation point towards a stretching sheet. They analysis carried out by them revealed that rate of heat transfer at the surface is an increasing function of the the magnetic field when the free stream velocity dominates the stretching velocity while, in the opposite case, the rate of heat transfer at the surface is a decreasing function of magnetic field. Bhattacharyya and Layek [9] studied the effect of external magnetic field on boundary layer flow of a nanofluid due to an exponentially permeable stretching sheet. Viscous and Joulean heating effects on the boundary layer nanofluid flow in the presence of homogeneous-heterogneous and non-linear convection, using the volume fraction model, was discussed by Nandkeolyar et al. [10].

The natural convection or free convection flow problem of a pure fluid over a vertical wall is a chaste problem on which several researchers have presented theoretical studies considering different aspects of the problem [11, 12]. The natural convection flow of a nanofluid over a stretching sheet with or without considering a porous medium were investigated by Nield and Kuznetsov [13] and Kuznetsov and Nield [14]. A theoretical investigation of the natural convective boundary layer flow of a nanofluid past a horizontal flat plate considering a porous medium was presented by Khan and Pop [15]. Chamkha and Aly [16] presented the numerical simulation of the steady magnetohydrodynamic natural convection nanofluid flow along a porous vertical wall. They observed that the local skin-friction coefficient behaves as increasing functions of thermophoresis parameter and nanoparticle Lewis number. Chamkha et al. [17] later presented a study investigating the flow properties of a non-Darcy free convective non-Newtonian nanofluid over a Cone. The study of thermal radiation effect s on the boundary layer flows were started probably way back in the year 1952 due its important effects in manufacturing industries for designing nuclear power plants and various engineering applications. It was perhaps Smith [18] who first studied the effect of thermal radiation on a boundary layer flow and thereafter a number of researchers presented the analytical/numerical analysis of boundary layer flows with thermal radiation effects. However the effect of thermal radiation on the flow of a nanofluid was only studied after the stimulus towards the study of nanofluid flows. The effects of radiative heat transfer on the mixed convection flow of a Newtonian nanofluid about a wedge and a cone saturated in a porous medium was studied by Chamkha et al. [19, 20]. In the above mentioned studies for considering the effect of radiation, the linearized form of Rosseland

approximation, which is valid only for small temperature differences between the ambient fluid and the fluid within the boundary layer, was used. However, Pantokratoras and Fang [21] later suggested that we could even use a nonlinear version of the Rosseland approximation for calculating the net heat flux due to radiation which remains valid even for large temperature differences between the ambient fluid and the fluid within the boundary layer. They applied this new idea on the classical Sakiadis flow over a moving plate. Ansari et al. [22] considered the magnetohydrodynamic viscoelastic nanofluid flow in the presence of nonlinear radiative heat transfer over a stretching sheet. They also included the effect of non-uniform heat generation/absorption in their study and found that the thermal radiation and non-uniform heat generation/absorption play vital role in controlling the temperature within the boundary layer region. The effect of non-linear thermal radiation on the stagnation point nanofluid flow towards a stretching sheet in the presence of homogneous-heterogeneous reactions was considered recently by Das et al. [23]. They used a numerical technique called spectral local linearization method to apply on the volume fraction model which was used to describe the nanofluid model. Mustafa et al. [24] presented a numerical solution using shooting technique for the problem of natural convection flow of a nanofluid over a flat plate with non-linear thermal radiation effects. The thermal boundary layer was found to be thickening with increasing effects of Brownian motion and thermophoresis diffusion.

In general, in most of the above research studies, the fluid flow problems have been solved under constant wall conditions. The fluid velocity at the wall is assumed to be a usual no-slip condition which, however in some cases, may not be valid. Especially in a fluid flow problem where the cohesive force is comparatively larger than the adhesive forces and in flows taking place at high altitudes, the assumption of the velocity-slip at the bounding surface becomes significant. Also, the fluid temperature in almost all the studies mentioned above is assumed to be having the temperature of the bounding surface which in a practical situation is not feasible and the transfer of heat follows Newton's law. Keeping all these arguments into mind, our study is based on the numerical analysis of hydromagnetic natural convection boundary layer flow of a nanofluid along a stretching sheet in the presence of non-linear thermal radiation, partial velocity-slip at the wall and Newtonian heating. The model involves the Brownian motion and thermophoresis diffusion terms to cater the presence of nanoparticles in the base fluid and the governing partial differential equations are solved numerically using the spectral relaxation method. The values of the coefficient of skin friction, heat and nanoparticle mass transfer are also obtained numerically to examine the various flow properties of the considered model.

2. MATHEMATICAL FORMULATION

We examine the natural convection boundary layer flow of a viscous, incompressible and electrically conducting nanofluid along a stretching sheet under the influence of a transverse variable magnetic field $B(x)$ of magnitude B_0 applied normal to the sheet. The $x-$axis is taken along the length of the sheet while the y-axis is normal to the sheet and hence parallel to the applied magnetic field. The sheet, which is convectively heated by a hot fluid of temperature T_f and heat transfer coefficient h_f, is stretched along the positive and negative directions of x-axis by two equal and opposite forces so that the origin O remains fixed. It is assumed that the magnetic Reynolds number of the fluid is vary small and thus, the induced magnetic field effects are negligible in comparison to the applied one. Further, it is assumed that the cohesive forces between the fluid molecules are comparatively

larger than the adhesive forces between the fluid molecules and the surface of the sheet. This causes a velocity slip at the surface of the sheet.

The partial differential equations governing the nanofluid flow and heat transfer, under the assumptions made above, are

$$\frac{\partial u}{\partial x}+\frac{\partial v}{\partial y}=0, \tag{1}$$

$$u\frac{\partial u}{\partial x}+v\frac{\partial u}{\partial y}=\nu\frac{\partial^2 u}{\partial y^2}-\frac{\sigma B^2(x)}{\rho_f}u+\frac{(1-C_\infty)\rho_{f\infty}\beta g(T-T_\infty)}{\rho_f}-\frac{(\rho_p-\rho_{f\infty})g(C-C_\infty)}{\rho_f}, \tag{2}$$

$$u\frac{\partial T}{\partial x}+v\frac{\partial T}{\partial y}=\alpha\frac{\partial^2 T}{\partial y^2}-\frac{1}{(\rho c)_f}\frac{\partial q_r}{\partial y}+\tau\left[D_B\frac{\partial C}{\partial y}\frac{\partial T}{\partial y}+\frac{D_T}{T_\infty}\left(\frac{\partial T}{\partial y}\right)^2\right], \tag{3}$$

$$u\frac{\partial C}{\partial x}+v\frac{\partial C}{\partial y}=D_B\frac{\partial^2 C}{\partial y^2}+\frac{D_T}{T_\infty}\frac{\partial^2 T}{\partial y^2}, \tag{4}$$

where u and v are the velocity components along the x and y axes, respectively, T and C, are respectively, temperature of the nanofluid and nanoparticle volume fraction, ν is the kinematic viscosity, σ is the electrical conductivity, ρ_f and ρ_p are density of base fluid and nanoparticles, respectively, g is acceleration due to gravity, α is the thermal diffusivity of the fluid, D_B is the Brownian diffusion coefficient, D_T is the thermophoretic diffusion coefficient and $\tau=\frac{(\rho c)_p}{(\rho c)_f}$ is the ratio of effective heat capacity of the nanoparticle material and heat capacity of the fluid with ρ being the density, c is the specific heat at constant pressure, the suffix ∞ denotes the values at the ambient fluid, and q_r denote the radiate heat flux.

The boundary conditions for the problem are

$$\begin{aligned}&u=U_w+N_1\nu\frac{\partial u}{\partial y}=ax+N_1\nu\frac{\partial u}{\partial y},\ v=0,\ -k\frac{\partial T}{\partial y}=h_f(T_f-T),\ C=C_w \text{ at } y=0,\\ &u\to 0,\ v\to 0,\ T\to T_\infty,\ C\to C_\infty,\ \text{as } y\to\infty,\end{aligned} \tag{5}$$

where $U_w=ax$ is the velocity at the sheet, k is thermal conductivity of the fluid, and N_1 is the hydrodynamic slip factor with dimension $(velocity)^{-1}$.

Following Pantokratoras and Fang [21], the radiative heat flux term is simplified as

$$q_r=-\frac{16\sigma^* T^3}{3\alpha^*}\frac{\partial T}{\partial y}, \tag{6}$$

where σ^* is the Stefan-Boltzmann constant, α^* is the Rosseland mean absorption coefficient.

In order to transform the governing equations into a similar form, we introduce the following dimensionless quantities

$$\begin{aligned}&\psi(x,y)=\alpha Ra_x^{1/4}f(\eta), u=\frac{\partial\psi}{\partial y},\ v=\frac{-\partial\psi}{\partial x},\ \theta=\frac{(T-T_\infty)}{(T_f-T_\infty)},\ \theta_r=\frac{T_w}{T_\infty},\ \phi=\frac{(C-C_\infty)}{(C_w-C_\infty)},\\ &\text{where } \eta=\frac{y}{x}Ra_x^{1/4},\end{aligned} \tag{7}$$

where $\theta_r = \frac{T_f}{T_\infty}$ is temperature ratio parameter, η is the dimensionless stream function, Ra_x is the local Rayleigh number defined as

$$Ra_x = \frac{(1 - C_\infty) g\beta(T_f - T_\infty)x^3}{\nu\alpha}. \tag{8}$$

The above transformation is chosen such that the equation of continuity (1) is automatically satisfied and the Eqs. (2), (3) together with (6), and (5), give us, respectively

$$f''' - Mf' + \frac{1}{4Pr}(3ff'' - 2f'^2) + \theta - Nr\phi = 0, \tag{9}$$

$$\left[1+\frac{4}{3N_R}\{1+(\theta_r-1)\theta\}^3\right]\theta''+\frac{3}{4}f\theta' + Nb\,\theta'\phi' + \left[Nt + \frac{4}{N_R}(\theta_r - 1)\{1 + (\theta_r - 1)\theta\}^2\right]\theta'^2 = 0, \tag{10}$$

$$\phi'' + \frac{3}{4}Lef\phi' + \frac{Nt}{Nb}\theta'' = 0. \tag{11}$$

The above set of equations is to be solved subject to the following boundary conditions:

$$\begin{aligned} &f(\eta) = 0,\ f'(\eta) = \lambda + Af''(\eta),\ \theta'(\eta) = -Nc[1 - \theta(\eta)],\ \phi(\eta) = 1 \text{ at } \eta = 0,\\ &f'(\eta) \to 0,\ \theta(\eta) \to 0,\ \phi(\eta) \to 0 \text{ as } \eta \to \infty. \end{aligned} \tag{12}$$

In the above equations and boundary conditions, the primes denote differentiation with respect to η and the other nine parameters are defined as

$$Pr = \frac{\nu}{\alpha},\ M = \frac{\sigma B^2}{\mu}\sqrt{\frac{x}{C_1}},\ C_1 = \frac{(1 - C_\infty)g\beta(T_f - T_\infty)}{\nu\alpha},\ Nr = \frac{(\rho_p - \rho_f)(C_w - C_\infty)}{\rho_f\beta(1 - C_\infty)},$$
$$Nb = \frac{\tau D_B(C_w - C_\infty)}{\alpha},\ Nt = \frac{\tau D_T(T_f - T_\infty)}{\alpha T_\infty},\ \lambda = \frac{ax^2}{\alpha\sqrt{Ra_x}},\ Le = \frac{\nu}{D_B},$$
$$Nc = \frac{h_f x^{1/4}}{k}\left[\frac{\nu\alpha}{(1 - C_\infty)g\beta(T_f - T_\infty)}\right]^{1/4},\ N_R = \frac{3K\alpha_*}{4\sigma_* T_\infty^3},\ A = \frac{N_1\nu Ra_x^{1/4}}{x},$$

where Pr is the Prandtl number, M is magnetic parameter, C_1 is dimensionless number, Nr is the buoyancy ratio parameter, Nb is the Brownian motion parameter, Nt is the thermophoresis parameter, λ is the stretching/shrinking parameter, Le is the Lewis number, Nc is the convective parameter, N_R is the thermal radiation parameter, and A is the momentum slip parameter.

The parameter Nc is found to be depending on x, and hence a true similarity is not achieved. In order to achieve a true similarity, we further assume that the convection heat transfer coefficient h_f is proportional to $x^{-1/4}$, as in such case Nc becomes independent of x. The convective parameter is related to the traditional Biot number and the Rayleigh number as

$$Nc = \frac{Bi_x}{Ra_x^{1/4}} \quad \text{where} \quad Bi_x = \frac{h_f x}{k}.$$

Apart from the velocity and temperature distribution within the flow field, in order to have an in-depth analysis of the physics of the problem, it would be interesting to look into the local skin-friction coefficient C_{f_x}, the local Nusselt number Nu_x and the local nanoparticle Sherwood number Sh_x. These are defined as

$$C_{fx} = \frac{\tau_w x^2}{\mu\alpha Ra_x^{3/4}}, \quad Nu_x = \frac{xq_w}{k(T_f - T_\infty)}, \quad Sh_x = \frac{xq_m}{D_B(C_w - C_\infty)},$$

where τ_w, q_w, and q_m are the wall shear stress, heat and mass fluxes, respectively, which are given by

$$\tau_w = \mu\left(\frac{\partial u}{\partial y}\right)_{y=0}, \quad q_w = -k\left(\frac{\partial T}{\partial y}\right)_{y=0} + (q_r)_{y=0}, \quad q_m = -D_B\left(\frac{\partial C}{\partial y}\right)_{y=0},$$

with μ and k being the dynamic viscosity and thermal conductivity of the fluid, respectively.

Using Eq. (7), we get

$$C_{f_x} = f''(0), \quad Ra_x^{-1/4}Nu_x = -\left[1 + \frac{4}{3N_R}\{1 + (\theta_r - 1)\theta(0)\}^3\right]\theta'(0), \quad Ra_x^{-1/4}Sh_x = -\phi'(0). \tag{13}$$

3. NUMERICAL SOLUTION

Eqs. (9)-(11) are nonlinear coupled ordinary differential equations which are to be solved subject to the boundary conditions prescribed in (12). The Spectral Local Linearization Method (SLLM) suggested by Motsa [25] and successfully employed by Shateyi and Gerald et al. [26] is used in the present paper to obtain numerical solution of the Eqs. (9)-(11) subject to the boundary conditions (12). The SLLM uses the idea of Gauss-Seidel approach for decoupling the system into a sequence of subsystem. The method then uses the Taylor Series expansion for local-linearization of each subsystem. Which in turn, gives a new decoupled system of linear equations. In the framework of SLLM, we obtained the following iteration scheme

$$f'_{r+1} = p_r, \tag{14}$$
$$p''_{r+1} + a_1 p'_{r+1} + a_2\, p_{r+1} = a_3, \tag{15}$$
$$b_1\theta''_{r+1} + b_2\theta'_{r+1} + b_3\theta_{r+1} = b_4, \tag{16}$$
$$\phi''_{r+1} + c_1\phi'_{r+1} = c_2, \tag{17}$$

where,

$$a_1 = \frac{3}{4Pr} f_{r+1}, \quad a_2 = -M - \frac{p_r}{Pr}, \quad a_3 = -\frac{1}{2Pr}p_r^2 - \theta_r + Nr\phi_r,$$
$$b_1 = 12N_R + 16 + 16(\theta_w - 1)^3\theta_r^3 + 48(\theta_w - 1)^2\theta_r^2 + 48(\theta_w - 1)\theta_r,$$
$$b_2 = 9N_R f_{r+1} + 12N_R Nb\phi'_{r+1} + 24N_R Nt\theta'_r + 96(\theta_w - 1)\theta'_r + 96(\theta_w - 1)^3\theta_r^2\theta'_r + 192(\theta_w - 1)^2\theta_r\theta'_r,$$
$$b_3 = 48(\theta_w - 1)^3\theta_r^2\theta''_r + 96(\theta_w - 1)^2\theta_r\theta''_r + 48(\theta_w - 1)\theta''_r + 96(\theta_w - 1)^3\theta_r\theta'^2_r + 96(\theta_w - 1)^2\theta'^2_r,$$

$$b_4 = 48(\theta_w-1)^3\theta_r^3\theta_r'' + 96(\theta_w-1)^2\theta_r^2\theta_r'' + 48(\theta_w-1)\theta_r\theta_r'' + 12N_R Nt\theta_r'^2 + 48(\theta_w-1)\theta_r'^2,$$
$$+ 144(\theta_w-1)^3\theta_r^2\theta_r'^2 + 192(\theta_w-1)^2\theta_r\theta_r'^2,$$
$$c_1 = \frac{3}{4}Lef_{r+1}, \quad c_2 = -\frac{Nt}{Nb}\theta_{r+1}''.$$

The boundary conditions for the above iteration scheme are

$$f_{r+1}(0) = 0, \tag{18}$$
$$p_{r+1}(0) = \lambda + Ap_{r+1}'(0), \qquad p_{r+1}(\infty) \to 0, \tag{19}$$
$$\theta_{r+1}'(0) = -Nc\{1-\theta_{r+1}(0)\}, \quad \theta_{r+1}(\infty) \to 0, \tag{20}$$
$$\phi_{r+1}(0) = 1, \qquad \phi_{r+1}(\infty) \to 0. \tag{21}$$

In order to solve the decoupled equations (14)-(17), we use the Chebyshev pseudospectral method. The computational domain $[0, L]$ is transformed to the interval $[-1, 1]$ using $\eta = L(\xi+1)/2$ on which the spectral method is implemented. Here L is used to invoke the boundary conditions at ∞. The basic idea behind the spectral collocation method is the introduction of a differentiation matrix $\mathcal{D}$ which is used to approximate the derivatives of the unknown variables at the collocation points as the matrix vector product of the form

$$\frac{df_{r+1}}{d\eta} = \sum_{k=0}^{N} \mathbf{D}_{lk} f_r(\xi_k) = \mathbf{D}\mathbf{f}_r, \qquad l = 0, 1, 2, \ldots, N, \tag{22}$$

where $N+1$ is the number of collocation points (grid points), $\mathbf{D} = $ ï‰2$\mathcal{D}/L$, and $\mathbf{f} = [f(\xi_0), f(\xi_1), \ldots, f(\xi_N)]^T$ is the vector function at the collocation points. Higher-order derivatives are obtained as powers of $\mathbf{D}$, that is,

$$f_r^{(p)} = \mathbf{D}^p\mathbf{f}_r, \tag{23}$$

where p is the order of the derivative.

Applying the spectral method to equations (14)-(17), we obtain

$$\mathbf{A}_1\mathbf{f}_{r+1} = \mathbf{B}_1, \qquad f_{r+1}(\xi_N) = 0, \tag{24}$$
$$\mathbf{A}_2\mathbf{p}_{r+1} = \mathbf{B}_2, \qquad p_{r+1}(\xi_N) = \lambda + Af''(\xi_N), \qquad p_{r+1}(\xi_0) = 0, \tag{25}$$
$$\mathbf{A}_3\Theta_{r+1} = \mathbf{B}_3, \qquad \theta_{r+1}(\xi_N) = -Nc\{1-\theta_{r+1}(\xi_N)\}, \ \theta_{r+1}(\xi_0) = 0, \tag{26}$$
$$\mathbf{A}_4\Phi_{r+1} = \mathbf{B}_4, \qquad g_{r+1}'(\xi_N) = 1, \qquad g_{r+1}(\xi_0) = 0, \tag{27}$$

where,

$$\mathbf{A}_1 = \mathbf{D}, \qquad \mathbf{B}_1 = p_r, \tag{28}$$
$$\mathbf{A}_2 = \mathbf{D}^2 + diag(a_1)\mathbf{D} + diag(a_2)\mathbf{I}, \qquad \mathbf{B}_2 = a_3, \tag{29}$$
$$\mathbf{A}_3 = diag(b_1)\mathbf{D}^2 + diag(b_2)\mathbf{D} + diag(b_3)\mathbf{I}, \qquad \mathbf{B}_3 = b_4, \tag{30}$$
$$\mathbf{A}_4 = \mathbf{D}^2 + diag(c_1)\mathbf{D}, \qquad \mathbf{B}_4 = c_2. \tag{31}$$

In equations (24)-(31), **I** is an identity matrix and $diag[\ ]$ is a diagonal matrix, all of size $(N+1)\times(N+1)$ where N is the number of grid points, **f**, **p**, Θ and Φ are the values of the functions f, p, θ and ϕ, respectively, when evaluated at the grid points and the subscript r denotes the iteration number.

The initial guesses to start the SRM scheme for equations (24)-(27) are chosen as

$$f_0(\eta)=\frac{A\lambda}{2}(1-e^{-\eta/A}),\quad p_0(\eta)=\frac{\lambda}{2}e^{-\eta/A},\quad \theta_0(\eta)=0.5e^{-\eta\ Nc},\quad g_0(\eta)=e^{-\eta}. \tag{32}$$

4. RESULTS AND DISCUSSION

In order to analyze the effects of the applied magnetic field, buoyancy-ratio, thermal radiation, Brownian motion, thermophoresis, temperature ratio, velocity slip, and the convective heating at the surface on the nanofluid velocity $f'(\eta)$, nanofluid temperature $\theta(\eta)$ and the nanoparticle concentration $\phi(\eta)$, the profiles of these quantities are depicted graphically in Figs. 1 - 8 for different values of the magnetic parameter (M), buoyancy-ratio parameter (Nr), thermal radiation parameter (N_R), Brownian parameter (Nb), thermophoresis parameter (Nt), temperature ratio parameter θ_r, velocity-slip parameter A, and the convective heating parameter Nc.

The effect of the magnetic parameter M which corresponds to the effect of the applied magnetic field is presented in Figure 1. The profiles of the nanofluid velocity, nanofluid temperature and the nanoparticle concentration for different values of the magnetic parameter is presented in this figure. It is observed that the nanofluid velocity decreases significantly with an increase in the applied magnetic field near to the plate in the boundary layer region. The fluid velocity overshoots its maximum value near the surface of the sheet away from the plate, and within the boundary layer region before approaching the free stream velocity, the fluid velocity increases with the increase in the strength of the magnetic field. However, the effect of the magnetic field is more significant near the surface of the sheet. The nanofluid temperature and the nanoparticle concentration experience increases with an increase in the magnetic field parameter.

Figure 2 presents the effect of the buoyancy ratio on the nanofluid velocity, nanofluid temperature and the nanoparticle concentration. Apart from the increasing effects on the nanofluid temperature and the nanoparticle concentration, the effect of the buoyancy ratio on the nanofluid velocity is more important to note. As in this case, the buoyancy ratio tends to decelerate the nanofluid velocity near the plate within the boundary layer region. The effect of buoyancy ratio is opposite in the boundary layer region close to the free stream.

The effect of the thermal radiation is presented in Figure 3. This is to be noted that the radiation effect is inversely proportional to the radiation parameter N_R. Thus, a small value of N_R corresponds to a large radiation effect and $N_R\to\infty$ corresponds to the case of zero radiation. It is evident from these figures that increasing the values of N_R causes decreases in the nanofluid velocity and the nanofluid temperature and an increase in the nanoparticle concentration. Thus, it may be concluded that the radiative heat transfer contributes in the thermal energy of the nanofluid which causes the nanofluid temperature to increase. The nanofluid velocity also increases with the increase in the movement of heated fluid particles from the higher temperature region to the lower temperature region. Also, an overshoot of the nanofluid velocity takes place near the surface of the sheet. This also causes the nanoparticle concentration to deceases in the boundary layer region.

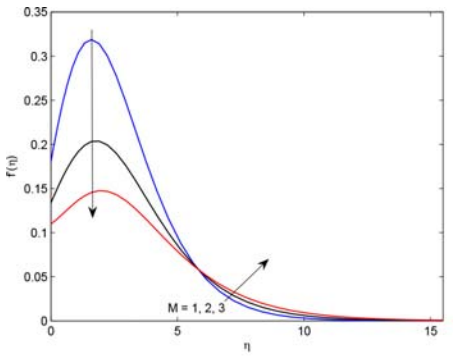

(a)

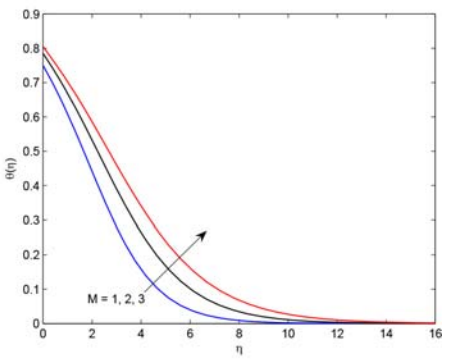

(b)

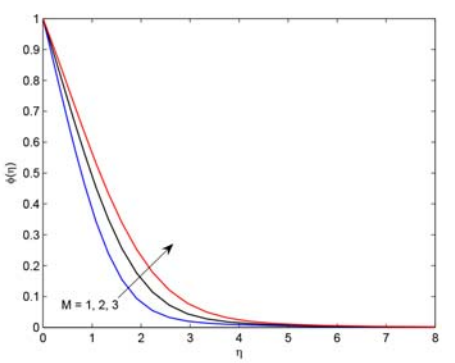

(c)

Figure 1. The effect of magnetic parameter M on (a) the fluid velocity f', (b) the fluid temperature θ and (c) species; concentration g when $Le = 5$, $Pr = 6.7850$, $Nr = 0.5$, $N_R = 5$, $Nb = 0.5$, $Nt = 0.5$, $\theta_r = 2$, $\lambda = 0.1$, $A = 0.5$ and $Nc = 0.5$.

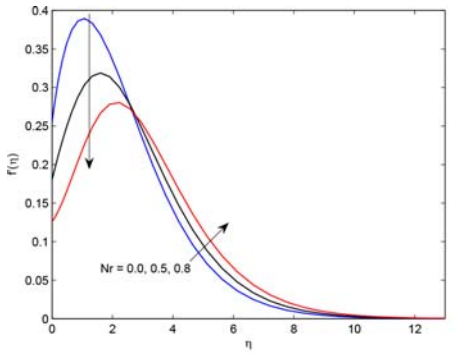

(a)

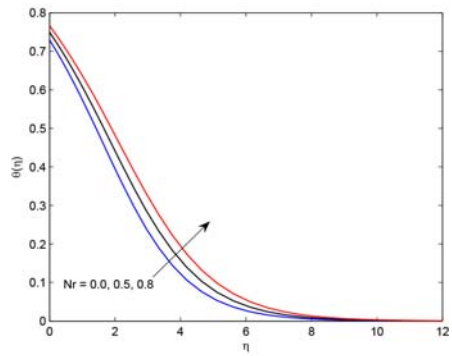

(b)

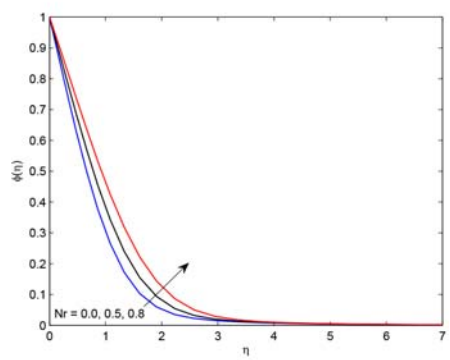

(c)

Figure 2. Variations in (a) f', (b) θ, and (c) g with respect to Nr when $M = 1$, $Le = 5$, $N_R = 5$, $Pr = 6.7850$, $Nb = 0.5$, $Nt = 0.5$, $\theta_r = 2$, $\lambda = 0.1$, $A = 0.5$, and $Nc = 0.5$.

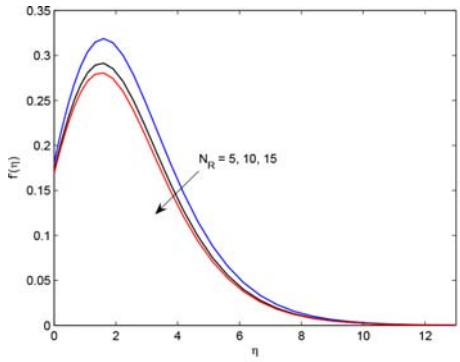

(a)

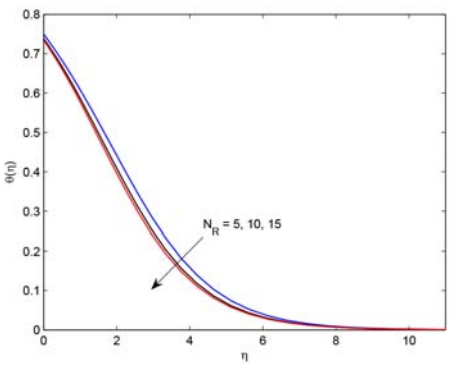

(b)

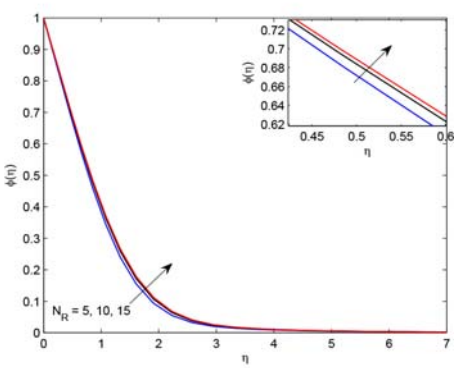

(c)

Figure 3. Variations in (a) f', (b) θ, and (c) g with respect to N_R when $Le = 5$, $M = 1$, $Pr = 6.7850$, $Nr = 0.5$, $Nb = 0.5$, $Nt = 0.5$, $\theta_r = 2$, $\lambda = 0.1$, $A = 0.5$, and $Nc = 0.5$.

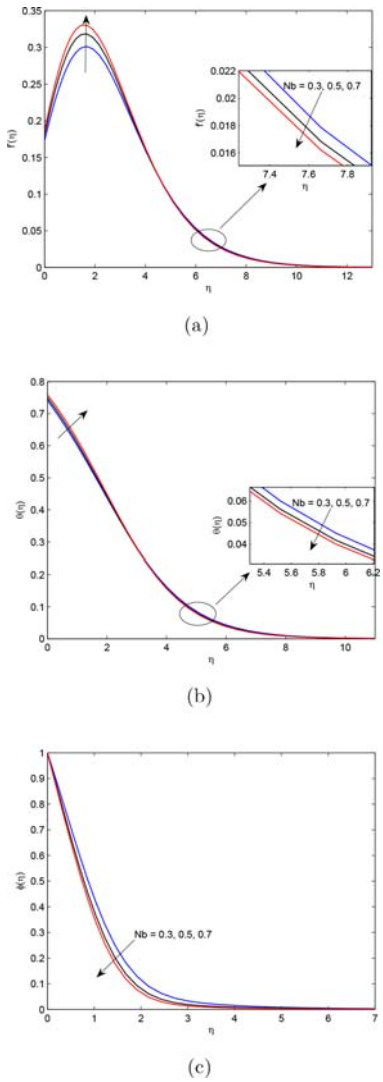

Figure 4. Variation in (a) f', (b) θ, and (c) g with respect to Nb when $Le = 5$, $M = 1$, $N_R = 5$, $Pr = 6.7850$, $Nr = 0.5$, $Nt = 0.5$, $\theta_r = 2$, $\lambda = 0.1$, $A = 0.5$, and $Nc = 0.5$.

Figure 4 presents the effect of Brownian motion on the nanofluid velocity, nanofluid temperature and the nanoparticle concentration. This effect is measured by an increase in the Brownian motion parameter Nb. It can be seen that the increase in the nanoparticle Brownian motion parameter causes increases in the nanofluid velocity and the nanofluid temperature near the surface within the boundary layer region. However, these can be seen decreasing in a region which is close to the ambient fluid. The nanoparticle concentration gets decreased by an increase in the Brownian

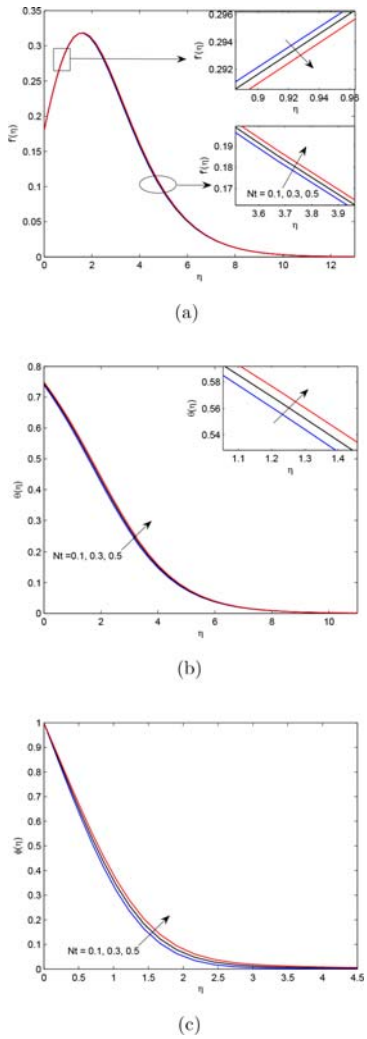

Figure 5. Variations in (a) f', (b) θ, and (c) g with respect to Nt when $Le = 5$, $M = 1$, $N_R = 5$, $Pr = 6.7850$, $Nr = 0.5$, $Nb = 0.5$, $\theta_r = 2$, $\lambda = 0.1$, $A = 0.5$, and $Nc = 0.5$.

motion parameter. The Brownian motion of the nanoparticle resulting from their collision with the molecules of the fluid tends to increase the fluid velocity and this also contributes in the thermal energy of the nanofluid. As a result of the Brownian motion, the nanoparticles tend to move away from the surface of the sheet which causes a decease in the nanoparticle concentration within the boundary layer region. In this figure, we also observe that the nanofluid velocity exceeds its maximum value near the surface of the sheet.

The effect of the thermophoretic force on the nanofluid velocity, nanofluid temperature and the nanoparticle concentration can be viewed in Figure 5. The thermophoratic force is the force

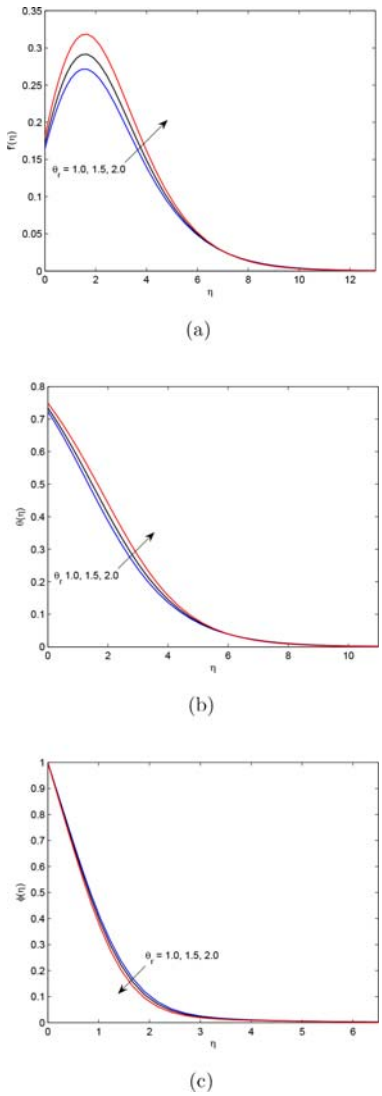

Figure 6. Variations in (a) f', (b) θ, and (c) g with respect to θ_r when $Le = 5$, $M = 1$, $N_R = 5$, $Pr = 6.7850$, $Nr = 0.5$, $Nb = 0.5$, $Nt = 0.5$, $\lambda = 0.1$, $A = 0.5$, and $Nc = 0.5$.

by which a nanoparticle pushes another nanoparticle away from the surface when the former gets heated due to the temperature of the sheet. It may be observed that the increase in the thermophoretic force causes a decrease in the nanofluid velocity near the sheet surface where as it has the reverse effect on the nanofluid temperature and the nanoparticle concentration throughout the boundary layer region. Figure 6 shows that the effect of the temperature ratio parameter $\theta_r (= \frac{T_f}{T_\infty} > 1)$ on the flow, heat and the nanoparticle mass transfer. Increasing values of $\theta_r (> 1)$ correspond to higher

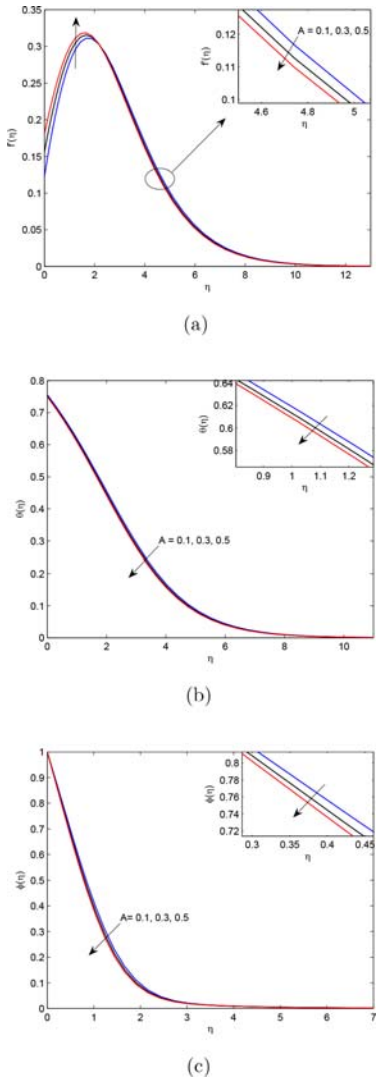

Figure 7. Variations in (a) f', (b) θ, and (c) g with respect to A when $Le = 5$, $M = 1$, $N_R = 0.5$, $Pr = 6.7850$, $Nr = 0.5$, $Nb = 0.5$, $Nt = 0.5$, $\theta_r = 2$, $\lambda = 0.1$, and $Nc = 0.5$.

surface temperatures and as a result of this, we observe an increase in the nanofluid velocity and the nanofluid temperature while a decrease in the nanoparticle concentration.

Figure 7 presents the variation in the profiles of the nanofluid velocity, nanofluid temperature and the nanoparticle concentration for various values of the slip parameter (A) which measures the relative slip between the fluid and the surface of the sheet. It is seen from Figure 7 that the nanofluid velocity increases near the surface while the nanofluid temperature and the nanoparticle

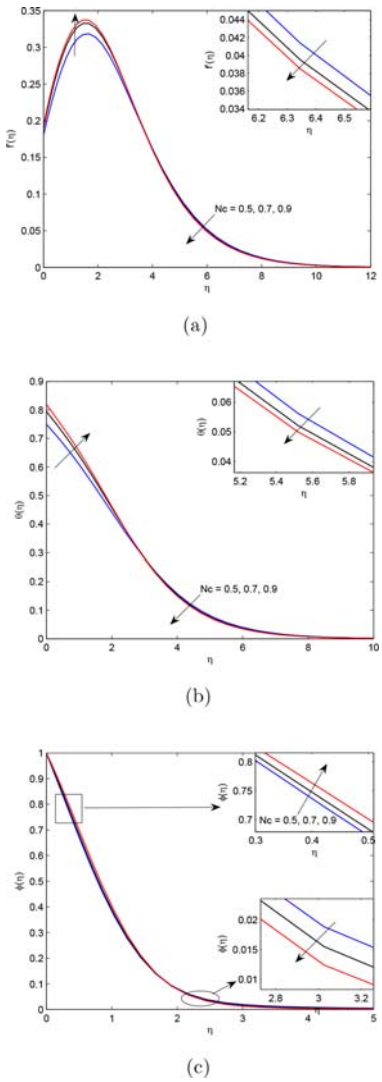

Figure 8. Variations in (a) f', (b) θ, and (c) g with respect to Nc when $Le = 5$, $M = 1$, $N_R = 5$, $Pr = 6.7850$, $Nr = 0.5$, $Nb = 0.5$, $Nt = 0.5$, $\theta_r = 2$, $\lambda = 0.1$, and $A = 0.5$.

concentration decrease with the increase in the slip between the fluid and the surface. The effect on the nanofluid velocity away from the surface is opposite in nature and the nanofluid velocity gets decreased with an increase in the slip velocity.

The profile of the nanofluid velocity, nanofluid temperature and the nanoparticle concentration for different values of the convective parameter (Nc) is presented in Figure 8. It is to be noted that an increase in the convective parameter signifies an increase in the Newtonian heating at the surface.

Table 1. Effects of various parameters on coefficient of local skin-friction, reduced local Nusselt number and Sherwood number when $Pr = 6.7850$, $Le = 5$, and $\lambda = 0.1$.

M	Nr	N_R	Nb	Nt	θ_r	A	Nc	C_{f_x}	$Ra_x^{-1/4} Nu_x$	$Ra_x^{-1/4} Sh_x$
1								0.16044827	0.30383121	0.64868914
2								0.06730899	0.27051328	0.50462127
3								0.0198231	0.25029851	0.4136204
	0							0.30942528	0.32177452	0.78018849
	0.5							0.16044827	0.30383121	0.64868914
	0.8							0.05202147	0.28805553	0.53226815
		5						0.16044827	0.30383121	0.64868914
		10						0.14406122	0.22221485	0.62279484
		15						0.13754038	0.19440772	0.61211764
			0.3					0.14526696	0.31111272	0.54969864
			0.5					0.16044827	0.30383121	0.64868914
			0.7					0.17132297	0.29548609	0.69578275
				0.1				0.16093264	0.31248787	0.74203381
				0.3				0.16077364	0.30807614	0.69543732
				0.5				0.16044827	0.30383121	0.64868914
					1			0.12862235	0.17488514	0.6000421
					1.5			0.1420935	0.22315965	0.6212633
					2			0.16044827	0.30383121	0.64868914
						0.1		0.21982592	0.29827668	0.59438524
						0.3		0.18558858	0.30150475	0.62596623
						0.5		0.16044827	0.30383121	0.64868914
							0.5	0.16044827	0.30383121	0.64868914
							0.7	0.17872131	0.3652654	0.60004141
							0.9	0.185694	0.42238509	0.53164104

The nanofluid velocity, nanofluid temperature and the nanoparticle concentration all gets increased near the surface with the increasing Newtonian heating, while in the later part of the boundary layer region, these all behave oppositely with the increase in Newtonian heating.

In Table 1, we present the effects of the magnetic parameter M, Buoyancy ratio parameter Nr, thermal radiation parameter N_R, Brownian motion parameter Nb, thermophoresis parameter Nt, temperature ratio parameter θ_r, velocity-slip parameter A, and the convective heating parameter Nc on the local coefficient of skin friction, local Nusselt number and local Sherwood number taking $Pr = 6.7850$, $\lambda = 0.1$ and $Le = 5$. The local skin friction coefficient C_{f_x} is found to be deceasing with increasing values of the magnetic field, buoyancy ratio, thermal radiation, themophoretic force and the velocity slip between the fluid and surface while it is oppositely affected by the Brownian motion parameter, temperature ratio, and the convective heating. The magnetic field, buoyancy ratio, thermal radiation, Brownian motion, and the thermophoretic force tend to reduce the local Nusselt number while the temperature ratio, velocity slip and the convective heating at the surface have increasing effects on it. The local Sherwood number which measures the rate of nanoparticle mass transfer from the surface, decreases with increases in magnetic field, buoyancy ratio, thermophoretic force, and the convecting heating, whereas it increases with increasing values of the Brownian motion parameter, temperature ratio and the slip-velocity parameter.

5. CONCLUSIONS

The natural convection boundary layer flow of a nanofluid over a stretching sheet under the influence of a magnetic field applied normal to the sheet is investigated numerically by employing the spectral local-linearization method with a view to highlight the effects of several parameters including the effects of non-linear thermal radiation, velocity slip, and Newtonian heating. The applied magnetic field and the buoyancy force appearing due to natural convection can be used as flow controlling agents which may delay the formation of the momentum boundary layer separation. The nonlinear thermal radiation and Newtonian heating at the surface contribute the thermal and kinetic energy of the fluid and increases the velocity and the temperature of the fluid significantly near the surface. The momentum slip i.e. the velocity slip has increasing effects on the nanofluid velocity whereas it has a retarding influence on the nanofluid temperature.

REFERENCES

[1] Choi SU and Eastman JA. Enhancing thermal conductivity of fluids with nanoparticles. Argonne National Lab., IL (United States); 1995 Oct 1.https://www.osti.gov/servlets/purl/196525/

[2] Choi SU, Zhang ZG, Yu W, Lockwood FE and Grulke EA, 2001. Anomalous thermal conductivity enhancement in nanotube suspensions. *Applied physics letters*. 79(14):2252–4.

[3] Xuan Y and Li Q, 2003. Investigation on convective heat transfer and flow features of nanofluids. *Journal of Heat transfer*. 125(1):151–5.

[4] Khan WA and Pop I, 2010. Boundary-layer flow of a nanofluid past a stretching sheet. *International Journal of heat and mass transfer*. 53(11-12):2477–83.

[5] Mustafa M, Hayat T, Pop I, Asghar S and Obaidat S, 2016. Stagnation-point flow of a nanofluid towards a stretching sheet. *International Journal of Heat and Mass Transfer*. 54(25-26):5588–94.

[6] Hassani M, Tabar MM, Nemati H, Domairry G and Noori F. An analytical solution for boundary layer flow of a nanofluid past a stretching sheet. *International Journal of Thermal Sciences*. 50(11):2256–63.

[7] Hamad MA, 2011. Analytical solution of natural convection flow of a nanofluid over a linearly stretching sheet in the presence of magnetic field. *International communications in heat and mass transfer*. 38(4):487–92.2.

[8] Ibrahim W, Shankar B and Nandeppanavar MM, 2013. MHD stagnation point flow and heat transfer due to nanofluid towards a stretching sheet. *International Journal of heat and mass transfer*. 56(1-2):1–9.

[9] Bhattacharyya K and Layek GC. Magnetohydrodynamic boundary layer flow of nanofluid over an exponentially stretching permeable sheet. Physics research international. http://downloads.hindawi.com/archive/2014/592536.pdf

[10] Nandkeolyar R, Motsa SS and Sibanda P, 2013. Viscous and Joule heating in the stagnation point nanofluid flow through a stretching sheet with homogenous–heterogeneous reactions and nonlinear convection. *Journal of Nanotechnology in Engineering and Medicine*. 1(4):4.

[11] Schmidt E and Beckmann W, 1930. Das Temperatur-und Geschwindigkeitsfeld vor einer Wärme abgebenden senkrechten Platte bei natürlicher Konvektion. *Technische Mechanik und Thermodynamik*. 1(11):391–406.

[12] Cheng P and Minkowycz WJ, 1977. Free convection about a vertical flat plate embedded in a porous medium with application to heat transfer from a dike. *Journal of Geophysical Research*. 82(14):2040–4.

[13] Nield DA and Kuznetsov AV, 2009. The Cheng–Minkowycz problem for natural convective boundary-layer flow in a porous medium saturated by a nanofluid. *International Journal of Heat and Mass Transfer*. 52(25-26):5792–5.

[14] Kuznetsov AV and Nield DA, 2010. Natural convective boundary-layer flow of a nanofluid past a vertical plate. *International Journal of Thermal Sciences*. 49(2):243–7.

[15] Aziz A, Khan WA and Pop I, 2012. Free convection boundary layer flow past a horizontal flat plate embedded in porous medium filled by nanofluid containing gyrotactic microorganisms. *International Journal of Thermal Sciences*. 56(1):48–57.

[16] Chamkha AJ and Aly AM, 2010. MHD free convection flow of a nanofluid past a vertical plate in the presence of heat generation or absorption effects. *Chemical Engineering Communications*. 198(3):425–41.

[17] Chamkha A, Abbasbandy S and Rashad AM, 2015. Non-Darcy natural convection flow for non-Newtonian nanofluid over cone saturated in porous medium with uniform heat and volume fraction fluxes. *International Journal of*

Numerical Methods for Heat & Fluid Flow. 25(2):422–437. http://citeseerx.ist.psu.edu/viewdoc/download?doi=10.1.1.708.8718&rep=rep1&type=pdf

[18] Smith JW, 1953. Effect of gas radiation in the boundary layer on aerodynamic heat transfer. *Journal of the Aeronautical Sciences*. 20(8):579–80.

[19] Chamkha AJ, Abbasbandy S, Rashad AM and Vajravelu K, 2012. Radiation effects on mixed convection over a wedge embedded in a porous medium filled with a nanofluid. *Transport in Porous Media.* 91(1):261–79.

[20] Chamkha AJ, Abbasbandy S, Rashad AM and Vajravelu K, 2013. Radiation effects on mixed convection about a cone embedded in a porous medium filled with a nanofluid. *Meccanica*. 48(2):275–85.

[21] Pantokratoras A and Fang T, 2012. Sakiadis flow with nonlinear Rosseland thermal radiation. *Physica Scripta*. 87(1):015703.

[22] Ansari MS, Nandkeolyar R, Motsa SS and Sibanda P, 2015. Viscoelastic Nanofluid Flow and Radiative Nonlinear Heat Transfer Over a Stretching Sheet. *Journal of Computational and Theoretical Nanoscience*. 12(9):2385-94.

[23] Das M, Mahatha BK and Nandkeolyar R, 2015. Mixed convection and nonlinear radiation in the stagnation point nanofluid flow towards a stretching sheet with homogenous-heterogeneous reactions effects. *Procedia Engineering*. 127(1):1018–25.

[24] Mustafa M, Mushtaq A, Hayat T and Ahmad B, 2014. Nonlinear radiation heat transfer effects in the natural convective boundary layer flow of nanofluid past a vertical plate: A numerical study. *PLoS One*. 9(9):e103946.

[25] Motsa SS, 2013. A new spectral local linearization method for nonlinear boundary layer flow problems. *Journal of Applied Mathematics*. 2013:423628. https://www.hindawi.com/journals/jam/2013/423628/abs/

[26] Shateyi S and Marewo GT, 2014. On a new numerical analysis of the Hall effect on MHD flow and heat transfer over an unsteady stretching permeable surface in the presence of thermal radiation and heat source/sink. *Boundary Value Problems*. 14(1):170.